Cathepsin S Controls the Trafficking and Maturation of MHC Class II Molecules in Dendritic Cells

Christoph Driessen,* Rebecca A.R. Bryant,* Ana-Maria Lennon-Duménil,* José A. Villadangos,* Paula Wolf Bryant,* Guo-Ping Shi,‡ Harold A. Chapman,‡ and Hidde L. Ploegh*

*Department of Pathology, Harvard Medical School, Boston, Massachusetts 02115; and ‡Department of Medicine, Brigham and Women's Hospital and Harvard Medical School, Boston, Massachusetts 02115

Abstract. Before a class II molecule can be loaded with antigenic material and reach the surface to engage CD4+ T cells, its chaperone, the class II-associated invariant chain (Ii), is degraded in a stepwise fashion by proteases in endocytic compartments. We have dissected the role of cathepsin S (CatS) in the trafficking and maturation of class II molecules by combining the use of dendritic cells (DC) from $CatS^{-/-}$ mice with a new active site–directed probe for direct visualization of active CatS. Our data demonstrate that CatS is active along the entire endocytic route, and that cleavage of the lysosomal sorting signal of Ii by CatS can occur there in mature DC. Genetic disruption of CatS dramatically reduces the flow of class II molecules to the cell surface. In $CatS^{-/-}$ DC, the bulk of major histocompatibility complex (MHC) class II molecules is retained in late endocytic compartments, although paradoxically, surface expression of class II is largely unaffected. The greatly diminished but continuous flow of class II molecules to the cell surface, in conjunction with their long half-life, can account for the latter observation. We conclude that in DC, CatS is a major determinant in the regulation of intracellular trafficking of MHC class II molecules.

Key words: major histocompatibility complex class II • cathepsins • dendritic cells • antigen presentation • biological transport

T lymphocytes use their antigen-specific receptors to recognize short fragments of antigenic proteins bound to the products of the major histocompatibility complex (MHC)[1] (Germain, 1994). MHC molecules occur in two major forms: class I products present peptides derived predominantly from cytosolic proteins, whereas class II products present antigenic fragments generated largely in the endocytic pathway (Heemels and Ploegh, 1995; Wolf and Ploegh, 1995). Antigen presentation by class II molecules relies on the confluence of their biosynthetic route with the endocytic pathway, which is richly endowed with proteases and other hydrolases that attack macromolecules, to ensure that even complex particulate matter will be converted into peptides presentable by class II products (Demotz et al., 1989a,b; Germain, 1994; Wolf and Ploegh, 1995; Chapman et al., 1997; Chapman, 1998).

The biosynthetic route traveled by class II molecules resembles that followed by most lysosomal membrane proteins (Ploegh, 1995; Pieters, 1997). The class II α and β subunits are assembled onto a scaffold of a trimeric type II membrane protein, the class II-associated invariant chain (Ii). Ii not only serves as a chaperone to facilitate the folding and assembly of class II molecules, but also contains the address code for their delivery to the endocytic pathway (Bakke and Dobberstein, 1990; Lotteau et al., 1990). The lumenal portion of Ii interacts with class II αβ dimers via a segment that binds in the peptide binding cleft, much in the manner of an antigenic peptide (Bijlmakers et al., 1994; Romagnoli and Germain, 1994; Ghosh et al., 1995). In the endocytic pathway, Ii is destroyed progressively by the combined action of cysteine and aspartyl proteases, culminating in the generation of a short Ii fragment referred to as CLIP (Roche and Cresswell, 1991; Newcomb and Cresswell, 1993; Maric et al., 1994; Amigorena et al., 1995; Riese et al., 1996; Villadangos et al., 1997; Chapman, 1998). For antigen presentation to occur, this fragment must be dislodged and exchanged for antigenic peptide in a reaction that is catalyzed by the MHC class II–like product, H2-DM (Denzin and Cresswell, 1995; Roche, 1995;

Address correspondence to Hidde L. Ploegh, Department of Pathology, Harvard Medical School, Building D2, 200 Longwood Ave., Boston, MA 02115. Tel.: (617) 432-4776. Fax: (617) 432-4775. E-mail: ploegh@mit.edu

J.A. Villadangos's present address is The Walter and Eliza Hall Institute, Royal Melbourne Hospital, Victoria 3050, Australia.

1. *Abbreviations used in this paper:* APC, antigen-presenting cell; CatS, cathepsin S; DC, dendritic cell(s); GM-CSF, granulocyte/macrophage colony-stimulating factor; Ii, class II-associated invariant chain; LAMP, lysosomal-associated membrane protein; LHVS, N-morpholinurea-homophenylalanyl-leucyl-vinylsulfonemethyl; M6PR, mannose-6-phosphate receptor; MHC, major histocompatibility complex; PDI, protein-disulfide isomerase; PhOH, phenol; PM, plasma membrane; PNS, postnuclear supernatant(s); TfR, transferrin receptor; wt, wild-type.

Sloan et al., 1995; Martin et al., 1996; Miyazaki et al., 1996). We have identified the cysteine protease cathepsin S (CatS) as a key enzyme in the conversion of Ii into CLIP (Riese et al., 1996, 1998; Villadangos et al., 1997; Shi et al., 1999). Inhibition of CatS halts processing of Ii at a stage referred to as Iip10, a fragment corresponding to the approximately NH_2-terminal 100 residues of Ii, extending from the very NH_2 terminus to the COOH terminus of CLIP (Villadangos et al., 1997; Nakagawa et al., 1999; Shi et al., 1999).

The potency of antigen-presenting cells (APCs) to present antigen appears to be linked both to the manner in which they handle class II trafficking (Cella et al., 1997) and to the sets of proteases to which newly internalized antigens are exposed (Chapman, 1998). This is perhaps best illustrated for dendritic cells (DC), the most potent professional APC. DC are now appreciated as a rather heterogeneous set of APCs depending on their provenance and history of exposure to cytokines (Banchereau and Steinman, 1998; Lotze and Thomson, 1999). Upon their maturation, DC undergo a dramatic redistribution of class II molecules to become strong stimulators of T lymphocytes (Cella et al., 1997; Pierre et al., 1997). The action of CatS was suggested as an essential element in this maturation process, because application of the CatS-selective inhibitor N-morpholinurea-homophenylalanyl-leucyl-vinylsulfonemethyl (LHVS) arrests class II molecules in a distribution characteristic of immature DC (Pierre and Mellman, 1998).

The lysosomal proteases are a set of enzymes of ever increasing complexity and new members of the thiol protease family with widely differing patterns of expression continue to be discovered (Chapman et al., 1997). Therefore, an important task is the assessment of the individual patterns of lysosomal protease activity encountered in distinct populations of professional APCs. These activities are relevant for maturation and trafficking of class II molecules as well as the generation of antigenic peptides from ingested microbes or soluble antigens (Chapman, 1998).

Here we resolve the complex role of CatS in the processing and intracellular trafficking of MHC class II molecules in DC by the combination of four tools: (a) the use of $CatS^{-/-}$ mice, thus eliminating the uncertainties inherent in any pharmacological manipulation; (b) the generation of DC by flt3 ligand treatment in vivo, which provides functionally mature DC in sufficient quantities for immunofluorescence and detailed biochemical analysis; (c) the combination of pulse–chase experiments with a cell fractionation scheme that resolves the major class II–containing endocytic compartments; and (d) the introduction of a new radiolabeled probe that allows direct visualization of enzymatically active CatS.

Materials and Methods

Mice

The $CatS^{-/-}$ (Shi et al., 1999) and $Ii^{-/-}$ (Viville et al., 1993) mice used here have been described; C57BL/6 mice (Jackson Laboratories) were used as wild-type (wt) controls. All animals were maintained under pathogen-free conditions at the animal facilities of Harvard Medical School in compliance with institutional guidelines.

Isolation of DC from Mice Treated with flt3 Ligand

Spleens were enriched in vivo with DC by stimulation with flt3 ligand (Maraskovsky et al., 1996). $CatS^{-/-}$, $Ii^{-/-}$, and C57BL/6 mice were subcutaneously injected with 4×10^6 flt3 ligand–secreting B16 melanoma cells (C57BL/6 background) prepared by transfection of murine flt3 ligand cDNA with the retroviral vector MFG (Shi et al., 1999). Spleen cells were harvested after the tumors reached 2–3 cm in diameter, at which time the spleens were 5–10-fold enlarged over those of untreated mice. A single-cell suspension of whole splenocytes was resuspended in a high-density BSA solution (4 ml per spleen) containing 10.6 g BSA (Intergen), 18.6 ml PBS, 2.9 ml 1 N NaOH, and 6.5 ml H_2O as described (Shi et al., 1999). After overlaying 2 ml of ice-cold RPMI, the splenocyte/BSA solution was centrifuged for 20 min at 9,500 *g*. About 5×10^7 DC per spleen were recovered from the interface and resuspended into RPMI. The cells were characterized by FACS using anti-B220, CD11c, CD11b, CD3, CD4, CD8, CD86, CD80, GR-1, and I-A^b antibodies. The surface phenotype of these cells, as revealed by extensive FACS analysis, did not differ significantly from the phenotype reported for DC generated by injection of the recombinant cytokine (Maraskovsky et al., 1996). Although this DC population is by no means homogenous with regard to its myeloid and/or lymphoid phenotype, it displays a uniform phenotype with regard to MHC class II surface expression, shows a robust antigen-presenting capacity in vitro (Shi et al., 1999), and therefore is considered as functionally mature DC (Maraskovsky et al., 1997; Shurin et al., 1997). Incubation of cells in either granulocyte/macrophage colony-stimulating factor (GM-CSF) or lipopolysaccharide (LPS) or both for up to 8 d did not lead to an increase in surface class II expression, and confirms the mature stage. Neither by FACS analysis nor light microscopy did we find any evidence for a maturation defect in $CatS^{-/-}$ DC. To assess the purity and confirm the phenotype of individual DC preparations, surface expression of I-A^b, B220, and CD11c was analyzed routinely by FACS for each experiment. For comparison of morphology and subcellular distribution of β-hexosaminidase, bone marrow–derived DC were generated by culturing bone marrow cells in GM-CSF for 6 d as described (Inaba et al., 1992). On day six, semiadherent clusters were isolated, purified on a 50% serum cushion, and allowed to mature in vitro by culturing them for 48 h.

Antibodies

N22, a hamster mAb that recognizes mouse MHC class II molecules (Metlay et al., 1990), was a gift from Dr. R.M. Steinman (Rockefeller University, New York, NY). The rabbit antiserum raised against the NH_2-terminal and the COOH-terminal regions of Ii (JV5: anti–NH_2 terminus, Ii 1–29; JV11: anti–COOH terminus, Ii 156–190) as well as the rabbit antiserum against murine protein-disulfide isomerase (PDI) were generated in our laboratory using standard techniques. Murine MHC class I molecules were retrieved with the p8 antiserum. Antibodies against murine transferrin receptor (TfR), LAMP-1 as well as fluorochrome-labeled antibodies against murine I-A^b, B220, CD80, CD86, CD11b, CD11c, CD8, and GR-1 were purchased from PharMingen. The rabbit antiserum against mannose-6-phosphate receptor (M6PR) was a gift from K.V. Figura (Max Planck Institute, Gottingen, Germany), the H2-DM antiserum was kindly provided by P. Pierre and I. Mellman (Yale University, New Haven, CT).

FACS Analysis

Single-cell suspensions were incubated for 30 min at 4°C with the appropriate conjugated antibodies in the presence of Fc Block (PharMingen), washed, and analyzed immediately on a FACScan (Becton Dickinson) using Cell Quest software.

Immunofluorescence

Freshly isolated cells (5×10^5) were plated in each well of glass chamber slides (Nalge Nunc International Laboratories) in complete RPMI medium supplemented with 20% FCS, and incubated at 37°C for 1 h to allow the cells to attach to the slide. All subsequent steps were performed at room temperature. Cells were washed once in PBS, and fixed for 20 min in a 3.7% solution of paraformaldehyde. After four washes in PBS, cells were permeabilized in RPMI medium containing 10% goat serum (GIBCO-BRL) and 0.05% saponin for 15 min. The primary and secondary antibody solutions were prepared in the same medium. Cells were incubated with the antibodies for 30 min and then washed three times. Slides were mounted in Aquapoly/Mount solution (Polysciences Laboratories) and analyzed in a Bio-Rad MRC 1024 confocal laser scanning mi-

croscope. The merged images were analyzed for the presence of class II–Ii molecules in LAMP-1 or DM positive structures using the colocalization program from Bio-Rad.

I-A^b molecules were detected using the Y3P antibody that recognizes mature αβ complexes and αβl, mouse Ii with the rabbit antisera JV5 and JV11. Secondary antibodies labeled with FITC were used for I-A^b and Ii detection. LAMP-1 was detected using a rat mAb (PharMingen) and a secondary antibody coupled to CY3. H2-DM was detected by the combination of rabbit anti-DM antiserum and an anti–rabbit antibody labeled with CY3. All secondary antibodies were made in goat and purchased from Jackson ImmunoResearch Laboratories.

Metabolic Labeling

Equal numbers of freshly prepared DC were incubated in 1 ml methionine/cysteine–free medium, supplemented with 10% FCS, 2 mM L-glutamine, penicillin (1:1,000 dilution U/ml), and 100 mg/ml streptomycin for 30 min. Cells were either continuously labeled with 0.5 mCi/ml [^{35}S]methionine/cysteine (80/20) (Dupont New England Nuclear) for 5 h or pulsed for 30 min and chased in 15 vol of complete RPMI supplemented with FCS, L-glutamine, penicillin, and streptomycin as above for the times indicated.

LHVS, synthesized as published (Palmer et al., 1995), was added to the pulse medium 20 min before the addition of [^{35}S]methionine/cysteine and the chase medium at a final concentration of 3 nM.

Subcellular Fractionation

Subcellular fractions were prepared essentially as described for murine B-lymphoblasts (Castellino and Germain, 1995); all steps were performed at 4°C. At each timepoint, cells were washed with PBS and 0.25 M sucrose, taken up in 2.2 ml homogenization buffer (0.25 M sucrose, 1 mM EDTA, pH 7.4, 1 mM PMSF), homogenized by six passes in a ball-bearing homogenizer (10-μm gap), and spun at 1,000 *g* for 10 min to obtain postnuclear supernatants (PNS). The amounts of incorporated [^{35}S]methionine/cysteine of the individual homogenates, as assessed by TCA precipitation, were adjusted to identical levels of radioactivity concentration with homogenization buffer. 9 ml of a 27% Percoll (Amersham Pharmacia Biotech) solution in 0.25 mM sucrose was layered on top of a 1-ml cushion of 2.5 M sucrose and overlaid with 2 ml of PNS (containing equal amounts of total incorporated radioactivity for each individual sample as described). After 1 h centrifugation at 34,000 *g* (4°C), 1-ml fractions were collected from the bottom of the tube. Fractions containing the low density peak of β-hexosaminidase activity (fractions 9 and 10) were pooled, applied to a 10% Percoll gradient, and fractionated by centrifugation as described for the 27% gradient.

Characterization of Subcellular Fractions

For both wt or Cat$S^{-/-}$ mice, the first gradient (27% Percoll) yielded two peaks of activity of the endocytic marker enzyme β-hexosaminidase (high density peak: fractions 1+2, referred to as peak A). To distinguish between early and late endosomal compartments, the low density peak of the β-hexosaminidase activity in the 27% Percoll gradient was applied to a subsequent 10% Percoll density gradient. This separation resulted in a predominant intermediate density peak of β-hexosaminidase activity at the bottom of the gradient, peak B (fractions 1+2 of the 10% gradient). Peak C (fractions 11+12) was defined based on distribution of radioactivity, although a small amount of β-hexosaminidase was detected reproducibly. This fractionation pattern, as assayed by the endocytic marker β-hexosaminidase, was not affected by the lack of CatS.

The marker profile showed that peak A contains mature lysosomes based on its density of 1.09 g/ml, its β-hexosaminidase activity, and the presence of the late endosomal and lysosomal marker LAMP-1. Nonlysosomal characteristics (the endosomal marker TfR and M6PR, the Golgi apparatus and ER markers galactosyl transferase and PDI, respectively, and MHC class I, which serves as a marker for surface expression) were absent from peak A.

The intermediate density peak of the 10% Percoll gradient (peak B) represents late endosomes (density 1.05 g/ml, positive for β-hexosaminidase, M6PR, and LAMP-1, but negative for TfR as well as for galactosyl transferase and PDI and MHC class I). The low density peak (peak C) consists of a mixture of compartments, namely ER–Golgi apparatus and early endosomes–plasma membrane (PM), in agreement with published observations (Castellino and Germain, 1995).

For every fraction of each individual experiment, the distribution of the endocytic marker β-hexosaminidase activity (Mane et al., 1989), was assayed as described (Rome et al., 1979). Similarly, quantification of total incorporated radioactivity in each fraction was routinely performed from TCA-precipitated material. Galactosyl transferase (Roth and Berger, 1982) was measured as published (Green et al., 1987). The distributions of TFR, LAMP-1, M6PR, and PDI (Mane et al., 1989) were visualized by Western blot using 100 μl of each fraction with the appropriate primary antibody and secondary antibody conjugated to peroxidase (Santa Cruz Biotechnology).

Immunoprecipitation

Immunoprecipitation experiments were performed as described (Villadangos et al., 1997).

Cell Surface Biotinylation and Immunoprecipitation

DC labeled in a pulse–chase experiment were washed three times in ice-cold PBS and incubated for 30 min at room temperature in PBS containing 0.5 mg/ml NHS-Sulfo-Biotin (Pierce). For each timepoint, the biotinylated cells were lysed in NP-40 lysis buffer, and class II molecules were immunoprecipitated with the N22 antibody. Staph A pellets were resuspended in 50 μl of PBS containing 1% SDS and boiled for 10 min. 1/10 of each precipitate was retained for later comparison with reimmunoprecipitates in SDS-PAGE. 1 ml lysis buffer containing 0.1% BSA was added to the remaining 9/10 of the precipitate. After centrifugation, the supernatant was precleared once, reimmunoprecipitated with streptavidin agarose beads as above, and analyzed by SDS-PAGE and autoradiography.

Densitometry

For quantitative evaluation, autoradiographs were analyzed using a Multi-Image Scanning Densitometer (Alpha Innotech) and the software provided by the manufacturer. Values for MHC class I, MHC class II α-chain,

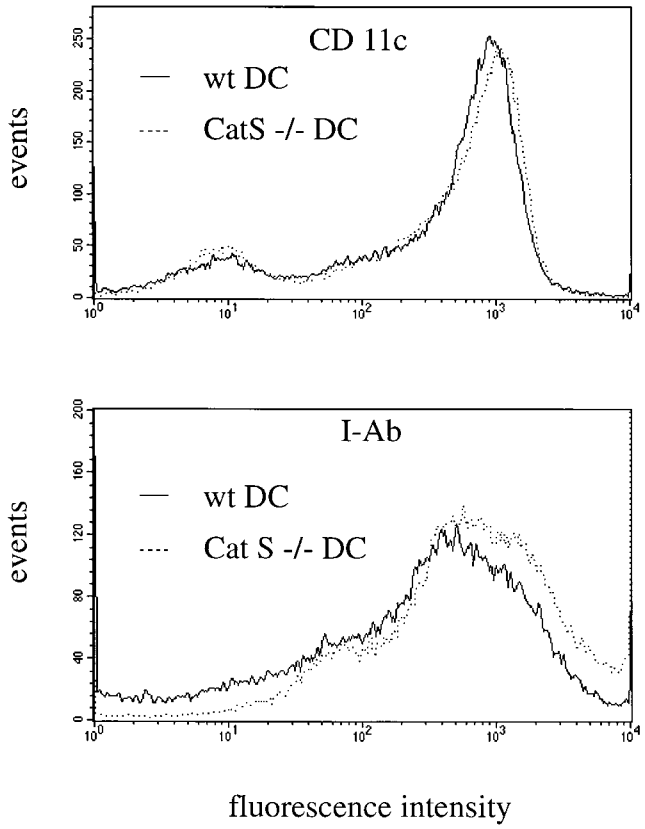

Figure 1. Surface expression of I-A^b molecules in wt and Cat$S^{-/-}$ DC. DC freshly prepared from flt3 ligand–induced wt and Cat$S^{-/-}$ splenocytes were stained with fluorochrome-labeled antibodies against I-A^b (MHC class II) and CD11c. Surface expression in the nongated live population was analyzed by FACS.

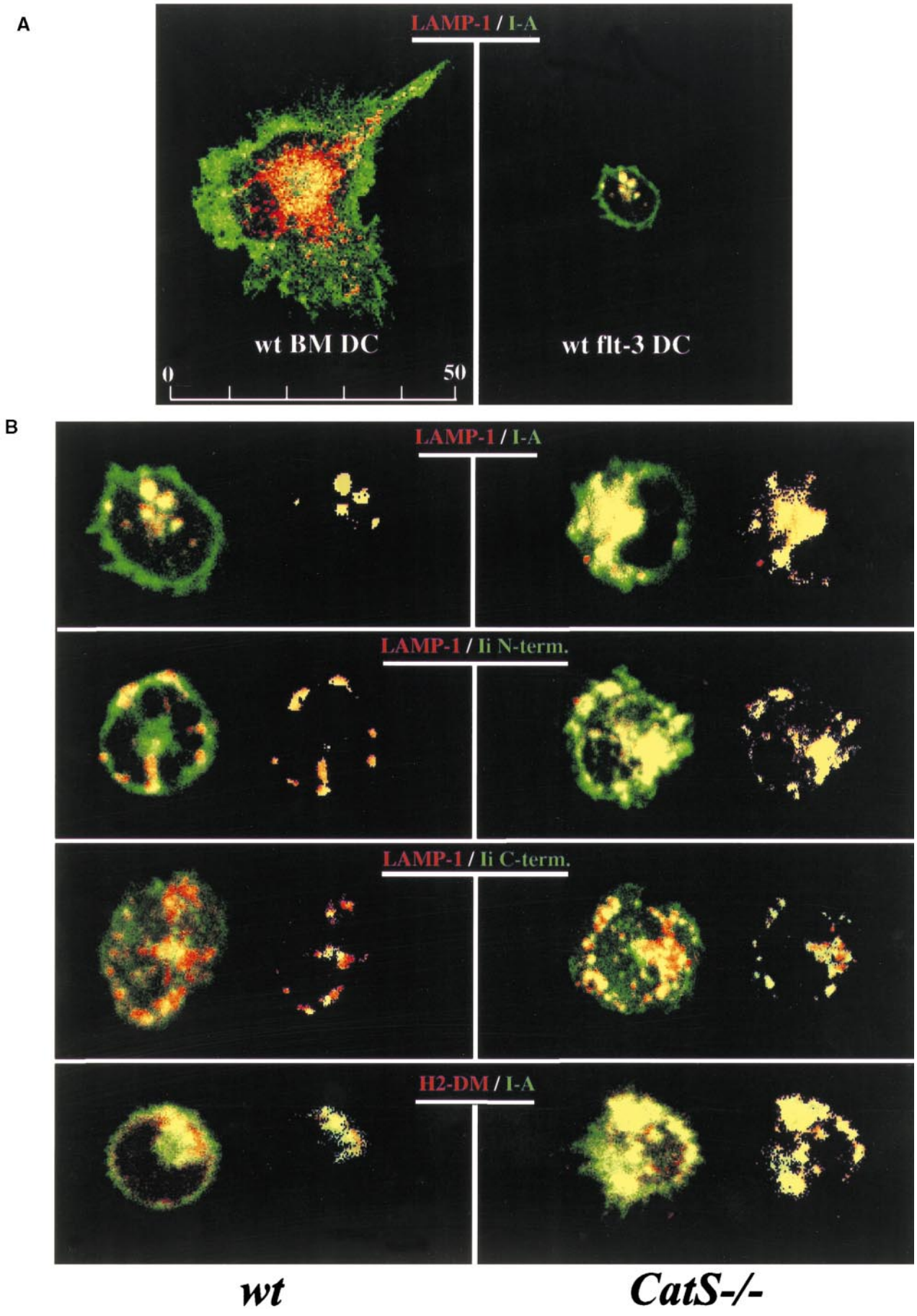

Figure 2 (continues on facing page).

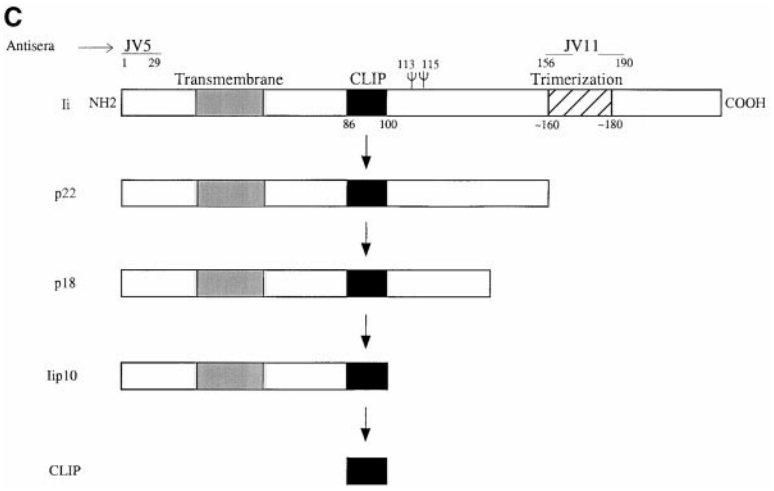

Figure 2. (A) Comparison of bone marrow–derived DC and DC induced by flt3 ligand treatment. Bone marrow–derived DC were generated by incubating bone marrow cells for 6 d in GM-CSF and were allowed to mature in culture for 48 h after purification of DC clusters (left). Flt3 ligand–induced DC were obtained from the spleen of mice injected with flt3 ligand–secreting melanoma cells. Both types of DC were permeabilized, stained for LAMP-1 (red) and class II molecules (green), and analyzed by confocal microscopy using identical magnification. (B) Intracellular localization of MHC class II, Ii, and H2-DM molecules in wt and CatS$^{-/-}$ DC. Freshly prepared flt3 ligand–induced DC from wt (left) and CatS$^{-/-}$ (right) mice were permeabilized and stained for the late endocytic marker LAMP-1 (red, top three rows), H2-DM (red, bottom row), and for MHC class II or Ii (green) (top and bottom rows, Y3P antibody against αβ dimers; second row, JV5 antiserum detecting the NH_2 terminus of Ii; third row, JV11 antiserum recognizing COOH-terminal portion of Ii). The merged image (left image) and the image resulting from the colocalization analysis (right image) are shown for both wt and CatS$^{-/-}$ DC. (C) Schematic view of Ii and its breakdown intermediates. MHC Ii is degraded intracellularly in a stepwise fashion. Three invariant chain molecules (Ii) bind in their trimerization region forming a homotrimer. Three αβ dimers assemble onto this scaffold of an Ii trimer, which results in the nonameric MHC class II complex $(\alpha\beta Ii)_3$ referred to as αβp (see also Fig. 6 A). This complex is disrupted by COOH-terminal proteolytic degradation of Ii by aspartyl and cysteine proteases including CatS, which leads to αβ molecules attached to degradation intermediates of Ii: p22, p18, and Iip10. In DC, NH_2-terminal degradation of Ii is performed by CatS, which converts Iip10 into CLIP. The epitopes recognized by the anti-Ii antisera are indicated (JV5, NH_2 terminus; JV11, COOH-terminal trimerization region).

SDS-stable dimers, and Ii breakdown intermediates were obtained by summing the respective background-corrected autoradiography signal corresponding to peak A, B, or C, either relative to each other (see Fig. 5) or in relation to the total amount of the particular species in the entire gradient (Fig. 3 and Fig. 4 A).

Active Site–Labeling of CatS with LHVS-Phenol

LHVS-phenol (PhOH) was synthesized following a scheme modified from that described (Palmer et al., 1995). ^{125}I–LHVS-PhOH (obtained by an Iodogen-catalyzed reaction) was purified further by reverse-phase HPLC. The peak fractions of radioactivity were dried down under reduced pressure and resuspended in DMSO. DC were washed three times with ice cold Hepes/RPMI. 1×10^6 cells were lysed for 2 h at 4°C in 100 μl lysis buffer (50 mM Tris, 5 mM $MgCl_2$, 0.5% NP-40, pH 7.4). Lysates and subcellular fraction samples (100 μl) were incubated with 10 nM ^{125}I–LHVS-PhOH at 37°C for 1 h (final DMSO concentration of 1.7–3%). Labeling was terminated by addition of 4× SDS sample buffer. The samples were boiled before analysis by 12.5% SDS-PAGE and visualization by fluorography.

Results

Intracellular Distribution of MHC Class II Molecules in Mice Lacking CatS

DC from CatS$^{-/-}$ mice and wt controls were generated by inoculation of the animals with flt3 ligand–secreting melanoma cells. Purified splenic DC were analyzed by FACS and confocal microscopy. Cells isolated from both types of animal consisted of ~80% B220^{low}, CD11c^{high}, MHC class II^{high} cells and therefore were judged to be DC, whereas the remainder were B cells and B220^{low} CD11c^{low} cells in roughly similar numbers. These cells were used for the experiments described here, and will be referred to simply as DC. Of note, significant morphological differences were detected when comparing flt3-induced splenic DC with DC generated from bone marrow precursors using GM-CSF (see Fig. 2 A). Flt3-induced DC are smaller in size and allow poorer resolution of intracellular compartments by microscopy. Furthermore, they show a different distribution profile of the endocytic marker β-hexosaminidase when compared with bone marrow–derived DC (see below).

Although class II surface expression was remarkably similar in CatS$^{-/-}$ and wt DC (Fig. 1 A), the intracellular distribution of class II was distinct, whereas no other gross morphological differences were detected (Fig. 2 B). We examined the steady-state distribution of class II molecules, Ii, and the late endocytic marker LAMP-1 by indirect immunofluorescence on freshly isolated and permeabilized DC. To detect class II molecules, the Y3P antibody was used; for detection of Ii, polyclonal antisera directed against the cytoplasmic tail of Ii (NH_2 terminus, JV5 antibody) or its lumenal region (COOH terminus, JV11 antibody) were used (Fig. 2 C). The staining for total class II molecules observed in CatS$^{-/-}$ DC is considerably enhanced compared with wt cells, suggesting that CatS activity influences the level of intracellular class II (Fig. 2 B). Colocalization of class II and LAMP-1 molecules showed that the fraction of class II in late endocytic structures is enhanced in CatS$^{-/-}$ DC. A similar observation was made when analyzing the colocalization of class II with H2-DM molecules (Fig. 2 B), confirming the increased fraction of class II antigens in late endocytic compartments from CatS$^{-/-}$ DC.

Similar results were obtained when using the JV5 antiserum directed against the NH_2-terminal portion of Ii (Fig. 2, B and C), suggesting that class II molecules in late endocytic compartments of CatS$^{-/-}$ DC are bound largely to Ii fragments that have retained an intact NH_2 terminus. To determine if these class II–Ii complexes contain intact Ii

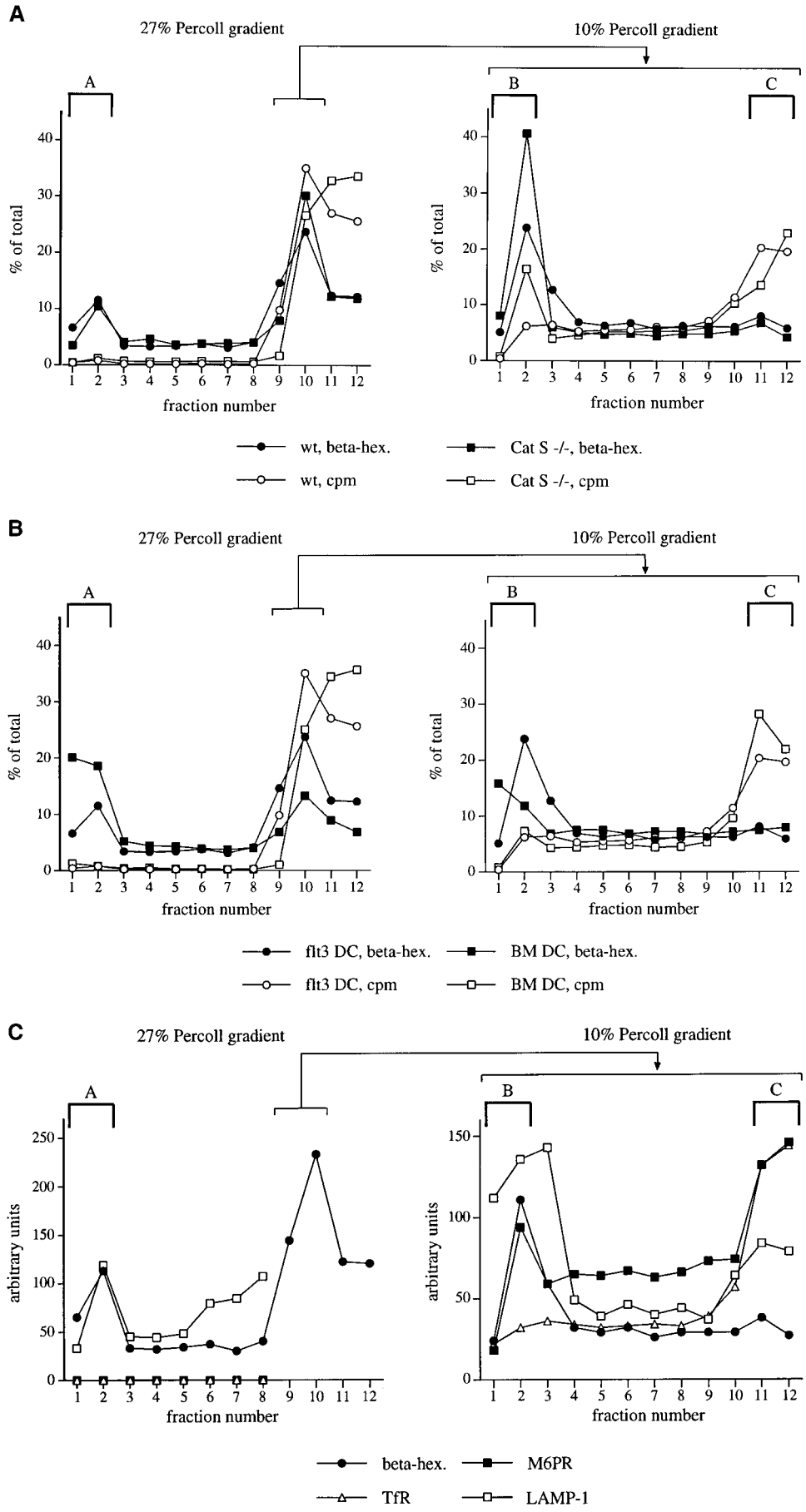

Figure 3. (A) Subcellular fractionation of flt3-induced DC from CatS$^{-/-}$ and wt mice. PNS of flt3-induced DC from CatS$^{-/-}$ and wt mice were fractionated using a 27% Percoll gradient as described, yielding the high-density peak A (left panel, fractions 1 and 2). The low-density peak of β-hexoaminidase activity (fractions 9 and 10) was applied subsequently onto a 10% Percoll gradient (right panel) to generate peaks B (fractions 1 and 2 of the 10% gradient) and C (fractions 11 and 12 of the 10% gradient). The β-hexosaminidase activity (beta-hex) and the distribution of incorporated radioactivity after metabolic labeling of the individual fractions are expressed as percentage of the total amounts retrieved from each gradient. (B) Comparison of the subcellular fractionation profiles from DC of different origin. DC from wt mice were either isolated from spleens after treatment with flt3 ligand (flt3 DC) or generated from bone marrow precursors of nontreated animals (BM DC). Subcellular fractions were prepared and assayed for β-hexosaminidase activity and incorporated radioactivity as in Fig. 3 A. (C) Characterization of subcellular fractions. Subcellular fractions were generated from flt3-induced splenic DC of wt mice as described. The distribution of lamp-1, M6PR, and TfR was assessed by Western blot followed by densitometry.

molecules, an antiserum that exclusively recognizes the p31 and p41 Ii forms (raised against the COOH-terminal part of Ii) (JV11; Fig. 2 C) was employed. No difference was seen in the extent of colocalization of LAMP-1 and Ii between wt and CatS$^{-/-}$ DC (Fig. 2 B). Thus, the MHC class II–Ii complexes that accumulate in late endocytic structures of CatS$^{-/-}$ DC must lack the COOH-terminal portion of Ii. As shown below, results from subcellular fractionation experiments are in agreement with this conclusion.

In all experiments, CatS$^{-/-}$ DC showed increased staining with Ii antibodies as compared with wt cells, indicating that the total intracellular amount of Ii is enhanced when CatS activity is absent (Fig. 2 B). Cytofluorometric analysis of CatS$^{-/-}$ and wt DC using the JV11 antiserum also revealed a significant increase of intact Ii at the surface of CatS$^{-/-}$ cells (data not shown). Finally, a stronger signal for LAMP-1 and H2-DM staining in CatS$^{-/-}$ compared with wt DC was consistently observed (Fig. 2 B).

In conclusion, the CatS$^{-/-}$ mutation leads to an accumulation of class II molecules bound to Ii with an intact NH_2 terminus in late endocytic compartments of mature DC. This observation is consistent with those obtained in LHVS-treated bone marrow–derived DC, resembles the intracellular distribution of class II in immature DC, and is most likely the result of incomplete cleavage of Ii in the absence of CatS. To verify this hypothesis and to determine the nature of the MHC class II–Ii complexes that accumulate in late endocytic compartments, subcellular fractionation experiments on CatS$^{-/-}$ and wt DC were performed.

Resolution of Three Distinct Endocytic Compartments in DC by a Two-Step Density Gradient Fractionation Scheme

Immunoelectron microscopy has shown that the majority of intracellular class II molecules in professional APC are found in conventional late endocytic structures (Kleijmeer et al., 1997). To resolve the major class II–containing compartments biochemically, DC from CatS$^{-/-}$ and wt animals were labeled with [^{35}S]methionine and subjected to subcellular fractionation. In brief, a homogenate was prepared using a ball-bearing–type homogenizer and the PNS was fractionated by two successive Percoll gradients. The first gradient (27% Percoll) allowed resolution of lysosomal fractions. This lysosomal peak will be referred to as peak A (Fig. 3, A and C). The unresolved material at the top of the 27% gradient was applied to a second gradient (10% Percoll), which yielded a high-density fraction enriched for late endosomes (peak B), and at low density, an unresolved peak comprising PMs, Golgi, early endosomes, and ER (peak C). No attempt was made to further resolve fraction C into its individual constituents. This fractionation scheme was used to characterize the subcellular distribution of CatS activity and to dissect trafficking and maturation of class II molecules in mature DC of wt and CatS$^{-/-}$ mice.

The modest activity of β-hexosaminidase in the lysosomal peak A appears to be a cell-specific trait. A direct comparison of the distribution profile of β-hexosaminidase activity between wt flt3-derived splenic DC and bone marrow–derived DC generated in GM-CSF reveals differences in the profile of the endocytic compartments for these two cell types. While the majority of β-hexosaminidase activity is found in the lysosomal compartment (peak A) in bone marrow–derived DC, this activity is distributed more towards the late endosomal compartment (peak B) with a relatively lesser amount in lysosomes in flt3-derived DC (Fig. 3 B).

Trafficking and Maturation of MHC Class II Molecules in wt and CatS$^{-/-}$ DC

Immunoprecipitations were performed with antibodies capable of recognizing class II molecules assembled with intact Ii as well as Ii intermediates. Assignment of Ii fragments was based on their reactivity with antipeptide antisera directed either against the cytoplasmic NH_2 terminus (antiserum JV5; see Fig. 2 C) or against the COOH-terminal trimerization domain (antiserum JV11) in conjunction with estimates of their molecular size and the presence or absence of N-linked glycans. For reference purposes, we performed subcellular fractionation on cells obtained from Ii$^{-/-}$ animals. In the absence of Ii, class II molecules assemble poorly and fail to be delivered efficiently to their normal destination. For all subcellular fractionations, the distribution of MHC class I molecules (H-2K^b) was examined as a representative protein largely excluded from endocytic compartments and unlikely to be affected in its intracellular trafficking by the absence of CatS. Fractionation experiments were conducted either on cells labeled continuously for 5 h (see Figs. 4 and 5) or in conjunction with pulse–chase labeling (see Figs. 6 and 8).

Analysis of the 27% Percoll gradients revealed that class II molecules in DC from Cat S$^{-/-}$ mice are more pronounced in their distribution over the lysosomal fraction and the denser regions of the gradient than in wt DC (Fig. 4 A). Furthermore, the overall recovery of class II molecules appears greater for the CatS$^{-/-}$ DC than for the wt DC, in agreement with the qualitative assessment by immunofluorescence (see Fig. 2 B). Class I products are recovered in approximately equal amounts and are distributed similarly in CatS$^{-/-}$ and wt DC (Fig. 4 B). As expected, in Ii$^{-/-}$ animals few if any class II molecules are recovered from the dense lysosomal fraction A (Fig. 4 B).

Analysis of fractions 9 and 10 obtained from the 27% Percoll gradient on a subsequent 10% Percoll gradient showed that in Cat S$^{-/-}$ DC, class II molecules accumulate in the late endosomal fraction with a very similar distribution to wt DC in the remaining portions of the gradient (Fig. 5 A). The distribution and recovery of MHC class I molecules from Cat S$^{-/-}$ DC is indistinguishable from wt cells (Fig. 5 B). As expected, class II molecules were not recovered from late endosomal fractions of Ii$^{-/-}$ DC (Fig. 5 B) (compare with both wt and CatS$^{-/-}$ DC).

The immunofluorescence in conjunction with the subcellular fractionation experiments showed that class II molecules accumulate intracellularly in DC from CatS$^{-/-}$ animals. The sites of intracellular accumulation are predominantly the late endosomes, and to a lesser extent, the lysosomes. Therefore, CatS regulates either the access of

class II molecules to, or the egress from, these compartments in flt3-induced splenic DC.

Next, we performed pulse–chase experiments in conjunction with the subcellular fractionation scheme outlined above (Fig. 6 A). The results from these experiments not only confirmed those obtained for continuously labeled cells, but also allowed important additional conclusions. By analysis of each of the immunoprecipitates under fully denaturing conditions (B; boiling in SDS sample buffer) as well as under more mildly denaturing conditions (NB; SDS sample buffer at room temperature), processing intermediates of Ii were recovered in a stable complex with the αβ heterodimer from different subcellular fractions. The sequence of events by which Ii is removed from class MHC class II–Ii complexes in wt and CatS$^{-/-}$ DC can thus be established.

Recovery and distribution of MHC class I molecules was relatively constant for the different chase points and did not differ between wt and CatS$^{-/-}$ DC (Fig. 6 A and Fig. 7 A). To quantitate the class II molecules themselves, the relative distribution of the class II α chain was analyzed. This parameter is valid because the N22 antibody used to recover class II molecules recognizes an epitope on the class II β subunit. The pattern of reactivity of N22 is generally assumed to be conformationally sensitive and dependent on proper heterodimer formation (Metlay et al., 1990).

After 30 min of labeling, class II molecules were visualized in CatS$^{-/-}$ and wt DC in peak C as SDS-stable complexes of ~100 kD, which represent the nonameric structure $(\alpha\beta Ii)_3$ referred to as αβp (Fig. 6 A, pulse). At this timepoint, almost all of the α chain carried high mannose-type oligosaccharides as indicated by its higher mobility compared with the mature form, which suggested that these molecules were still located in the ER–Golgi. This

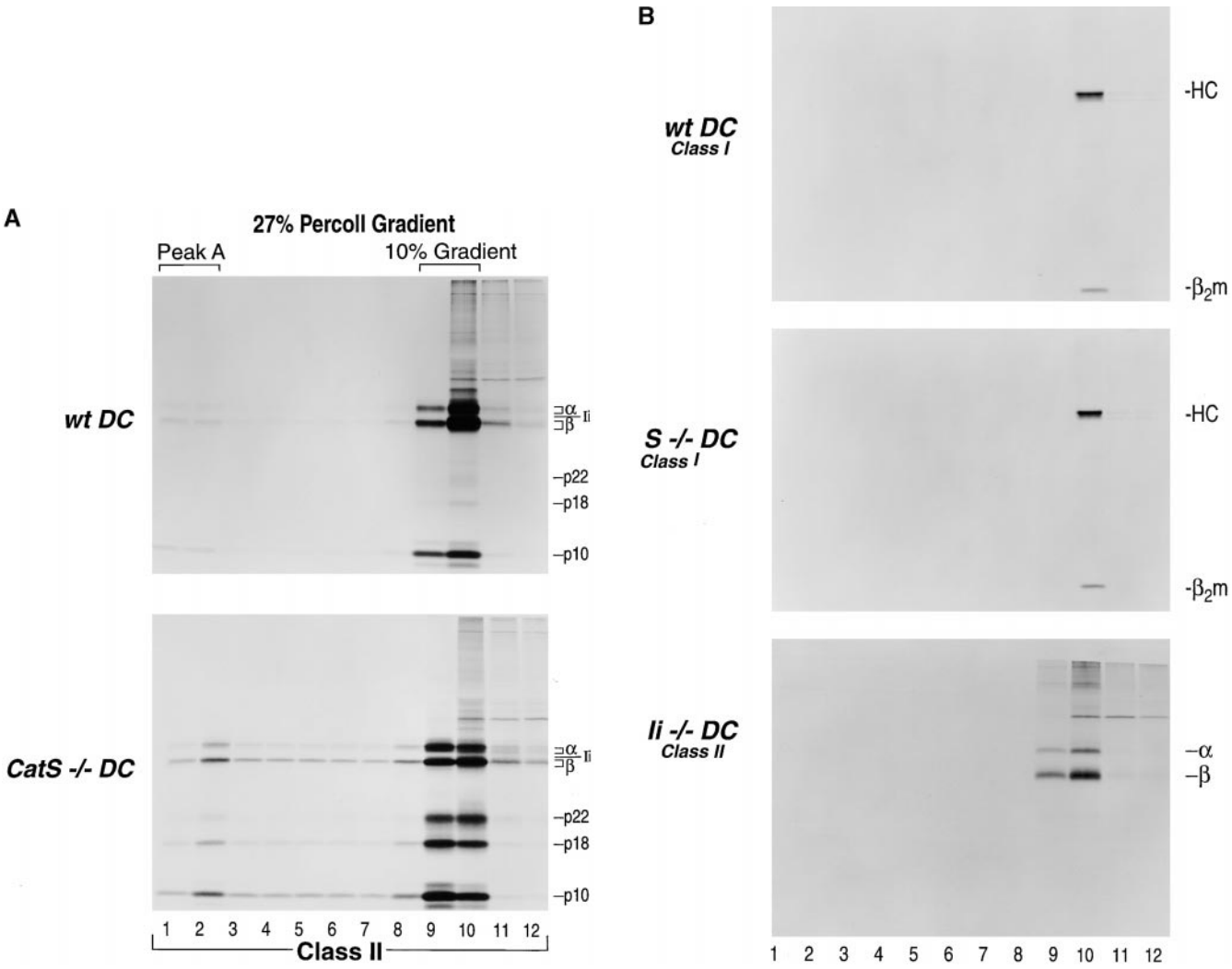

Figure 4. Steady-state distribution of MHC class II molecules after fractionation of wt and CatS$^{-/-}$ DC on a 27% Percoll gradient. DC were continuously labeled for 5 h, homogenized, and PNS were fractionated over a 27% Percoll gradient. 1-ml fractions were collected from the bottom of the tube and analyzed by immunoprecipitation, followed by boiling of the samples, 12.5% SDS-PAGE, and autoradiography. (A) Immunoprecipitation for MHC class II dimers from DC from wt and CatS$^{-/-}$ mice, using the N22 antibody (α/β: MHC class II α/β chain; Ii: invariant chain; p22, p18, p10: breakdown intermediates of Ii of the estimated molecular weight indicated). (B) Same subcellular fractions immunoprecipitated for MHC class I with the p8 antiserum (top and middle panels) (HC, class I heavy chain; β_2m, β-2 microglobulin). (Lower panel) Identical experiment performed with DC from Ii$^{-/-}$ mice and immunoprecipitated with N22.

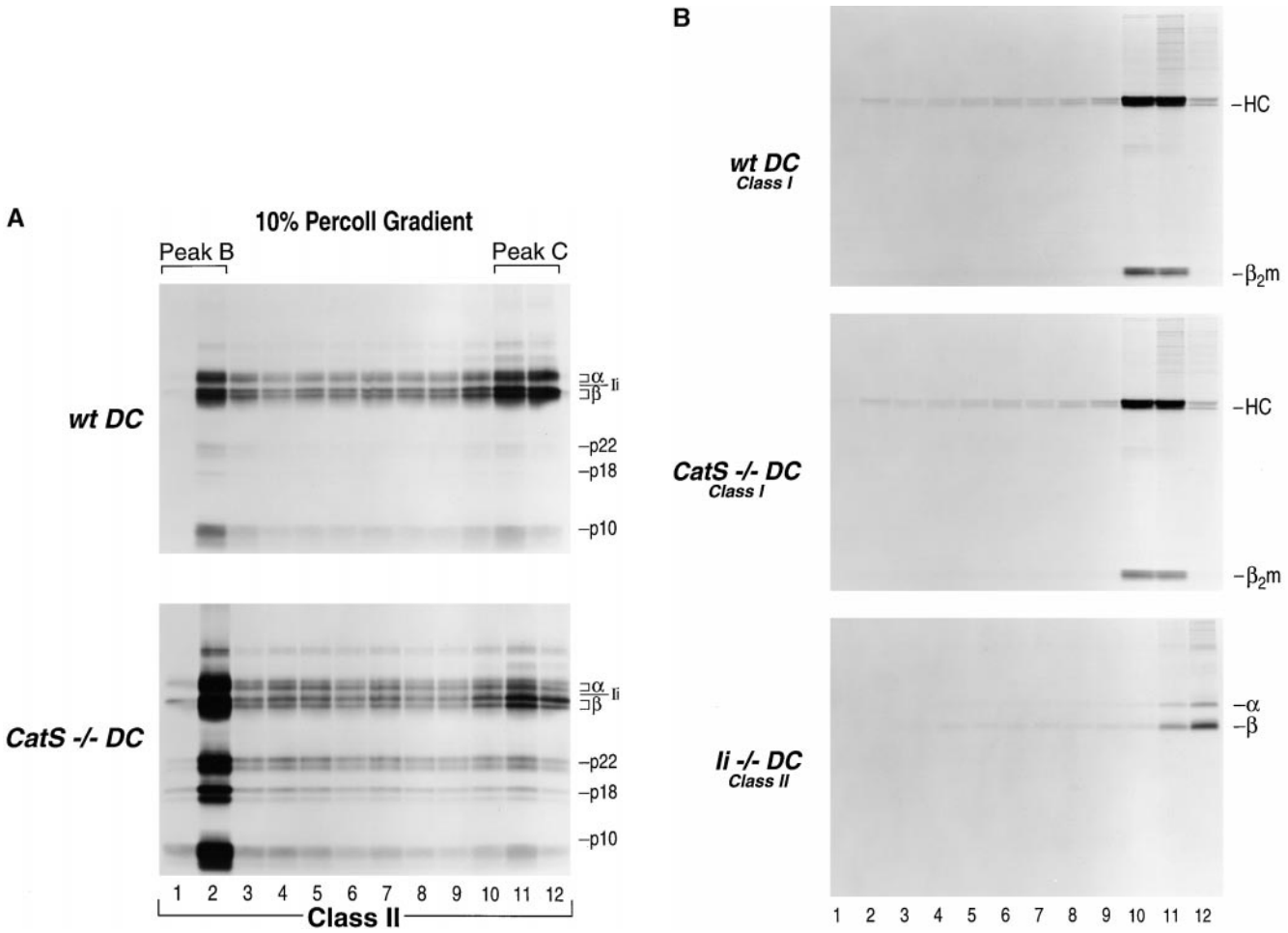

Figure 5. Steady-state distribution of MHC class II molecules after fractionation of wt and CatS$^{-/-}$ DC on consecutive 27 and 10% Percoll gradients. Fractions 9 and 10 from the 27% Percoll gradient (Fig. 4) were applied to the second gradient (10% Percoll) to separate late endosomes from the remainder. 1-ml fractions were collected from the bottom of the tube and analyzed by immunoprecipitation, followed by boiling of the samples, 12.5% SDS-PAGE, and autoradiography. (A) Immunoprecipitation with N22 for MHC class II dimers (α/β, MHC class II α/β chain; Ii, invariant chain; p22, p18, and p10, breakdown intermediates of Ii of the estimated molecular weight indicated). (B) Immunoprecipitation for MHC class I with the p8 antiserum from the same fractions as 5a (top and middle) (HC, class I heavy chain; β2m, β-2 microglobulin). (Lower panel) Identical experiment performed with DC from Ii$^{-/-}$ mice and immunoprecipitated with N22.

αβ–Ii complex appeared in peak B in both cell types at later timepoints, but the α chain was in its mature, fully glycosylated form.

After 1 h of chase, class II molecules reached endocytic compartments, and were transformed into ~70 kD αβl complexes by COOH-terminal degradation of Ii. No differences in either the kinetics or the subcellular distribution of αβl complexes were seen between wt and CatS$^{-/-}$ DC. This suggests direct trafficking from the ER–Golgi to early as well as late endosomes upon maturation of class II molecules, and demonstrates that access of class II complexes to late endosomes is independent of CatS activity.

Comparison of the 1 and 3 h chase points immediately revealed the progression of class II molecules from endocytic compartments to the peak that includes the PM (peak C) in wt DC, whereas in CatS$^{-/-}$ DC a greater fraction of class II molecules was arrested in late endocytic fractions (Fig. 6 A, peaks A and B; and Fig. 7 B). As expected, in wt DC the accumulation of mature, peptide-loaded class II molecules increased with time, and was most pronounced in lysosomes (peak A) and at the cell surface (Fig. 6 A and Fig. 7 C). The difference in intensity between the signal retrieved for mature class II complexes at the cell surface and its adjoining intracellular compartments (late endosomes) was striking, and suggested that none of these compartments could solely account for the total amount of class II complexes that finally reach the cell surface. In contradistinction, no fully mature αβ–peptide complexes can be detected after a 3-h chase in CatS$^{-/-}$ DC (Fig. 6 A and Fig. 7 C).

Of note, the αβl isoform of class II, which is converted into class II–CLIP complexes by CatS, was detected along the entire endocytic route in wt DC. This raised the possibility that the activity of CatS might show a similar subcellular distribution. We addressed this aspect by active site–labeling of CatS, shown below.

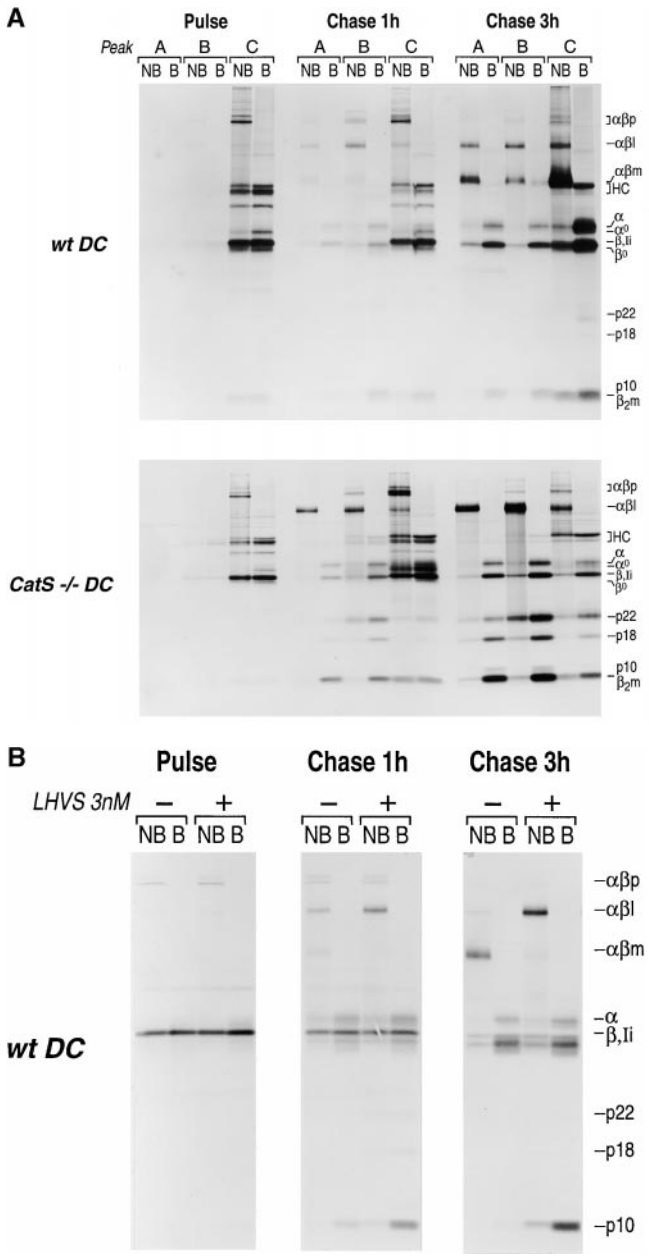

Figure 6. (A) Subcellular distribution of MHC class II molecules in wt and CatS$^{-/-}$ DC under pulse chase-labeling conditions. Flt3-induced DC from wt (upper panel) and CatS$^{-/-}$ (lower panel) mice were metabolically labeled with [^{35}S]methionine/cysteine for 30 min (pulse) and chased for 1 and 3 h. At each timepoint, subcellular fractions A (lysosomes), B (late endosomes), and C (early endosomes/PM and ER–Golgi) were generated as described. Immunoprecipitation from these fractions was performed with N22 (class II) and p8 (class I) at the same time. The samples were divided into two and analyzed by 12.5% SDS-PAGE either without (NB) or with prior boiling (B). (αβp, high molecular weight nonameric $[\alpha\beta Ii]_3$ complexes; αβl, 70-kD SDS-stable complex consisting of αβ bound to the Ii degradation intermediates Ii-p10, Ii-p18, or Ii-p22; αβm, mature SDS-resistant αβ dimer bound to either CLIP or peptide; HC, MHC class I heavy chain; α, mature class II alpha chain; α^0, immature α chain; β, mature β-chain; Ii, full-length invariant chain; β^0, immature β-chain; p10/p18/p22, COOH-terminal degradation intermediates of Ii; β_2m, β-2 microglobulin). (B) Effect of LHVS on the degradation of Ii in mature wt DC. DC were metabolically labeled for 30 min, and chased for 0, 1, or 3 h as described, either in the presence (+) or the absence (–) of the CatS inhibitor LHVS at 3 nM concentration. Cell lysates were prepared without any further subcellular fractionation steps and directly analyzed by immunoprecipitation using the N22 antibody. After separation by 12.5% SDS-PAGE with (B) or without prior boiling of the samples (NB), the samples were visualized by autoradiography.

In wt DC only the Iip10 form accumulated to easily detectable levels, whereas the p22 and p18 forms of Ii were not readily detected (Fig. 6 A and Fig. 7 D). In CatS$^{-/-}$ DC, Ii intermediates were more prominent at 3 h of chase than after 1 h. In absolute amounts, late endosomes contained the largest quantities of Ii breakdown intermediates (Fig. 6 A and Fig. 7 D). Interestingly, in late endosomes the p22 intermediate was more abundant than p18, whereas in lysosomes p22 was less abundant than p18 (Fig. 6 A and Fig. 7 D). In peak C, which based on the presence of TfR includes early endosomes, the p22 to p18 ratio was even higher than in peaks A (lysosomes) and B (late endosomes). These findings are consistent with a precursor–product relationship for p22 and p18, where the most likely sites of conversion are late endosomes and lysosomes.

In contrast to CatS$^{-/-}$ DC, only accumulation of Iip10, but not of p22 and p18, was observed when the CatS activity in wt DC was pharmacologically inhibited by incubation with LHVS (Fig. 6 B), although conversion from αβl to αβm is efficiently blocked by this inhibitor. This suggests that LHVS, even at 3 nM, might not completely block CatS activity, i.e., p22 and p18 were still degraded by CatS in the presence of LHVS, although Iip10 did accumulate.

Combined, these data suggest that in CatS$^{-/-}$ DC, the maturation of class II molecules is severely compromised due to a failure to process Ii properly. Breakdown intermediates of Ii remain associated with class II molecules, which accumulate intracellularly in late endosomes and lysosomes. In view of the similar steady-state levels of class II molecules at the cell surface of wt and CatS$^{-/-}$ DC, the flux of class II molecules from the endocytic pathway to the cell surface must be strongly inhibited in CatS$^{-/-}$ DC.

Kinetics of MHC Class II Surface Expression in wt and CatS$^{-/-}$ DC

The surface deposition of class II molecules was measured more directly for wt and CatS$^{-/-}$ DC by performing surface biotinylation in conjunction with pulse–chase analysis (Fig. 8). Only surface-disposed radiolabeled class II molecules that arrive over the course of a pulse–chase will become a substrate for surface biotinylation and allow their recovery on a streptavidin–agarose matrix. In wt DC, we observed extensive maturation of class II molecules over a 3-h and overnight chase, as inferred from the accumulation of SDS-stable, fully mature αβ–peptide complexes. Of these molecules, a fraction can be surface biotinylated, and this fraction increased very little between the 3-h and overnight chase timepoints. Although surface biotinylation is not quantitative, the data suggest that deposition of class II molecules on the cell surface reached a plateau at or shortly after 3 h of chase in wt DC. In CatS$^{-/-}$ DC, we

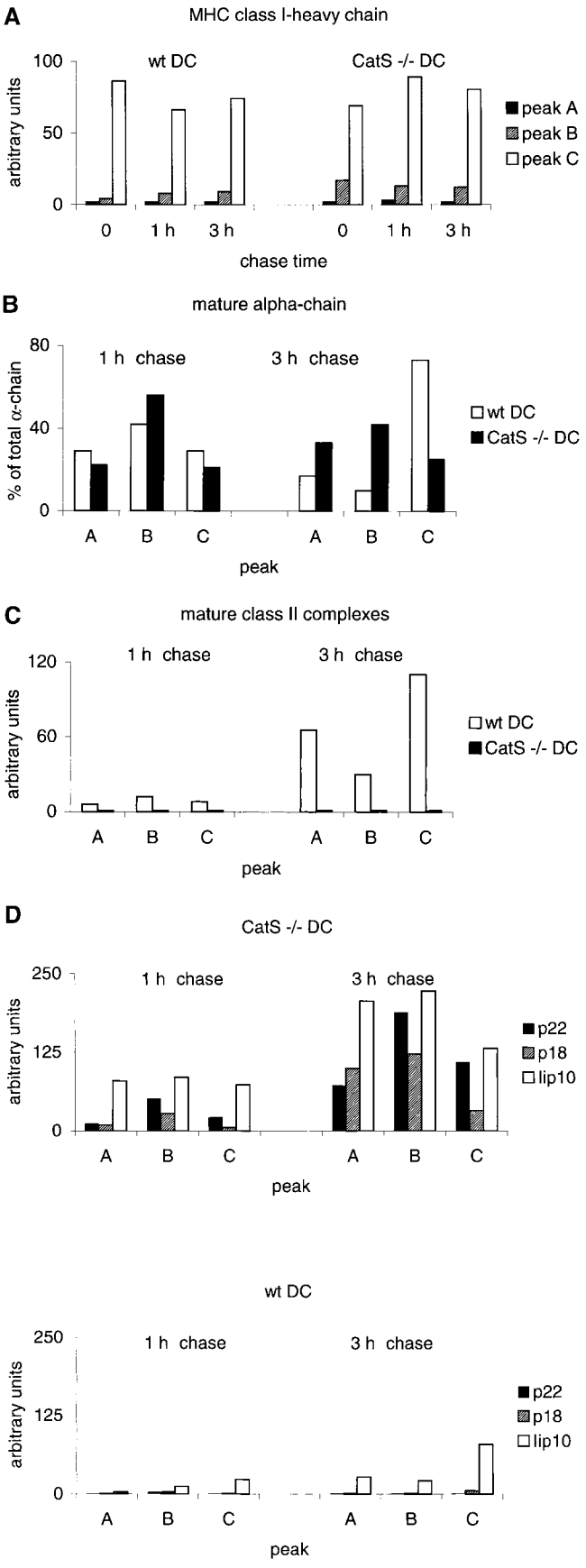

Figure 7. Quantitative assessment of trafficking and maturation of MHC molecules in wt and CatS$^{-/-}$ DC. Signals corresponding to individual polypeptides from Fig. 6 A were quantified by densitometry and plotted to assess the maturation and subcellular distribution of MHC class II molecules in DC from wt and CatS$^{-/-}$ mice. (A) Trafficking of MHC class I heavy chain in wt and CatS$^{-/-}$ DC. (B) Trafficking of total MHC class II molecules in wt and CatS$^{-/-}$ DC. The signal retrieved from the mature α-chain in relation to the signal from total α-chain was plotted. (C) Subcellular distribution of mature MHC class II complexes (αβm) in wt and CatS$^{-/-}$ DC. (D) Subcellular distribution of the Ii degradation intermediates p22, p18, and Iip10 in DC from wt and CatS$^{-/-}$ mice.

observed the accumulation of the αβl complex at 3 h and after overnight chase, whereas very little material was accessible to surface biotinylation. Therefore, the flux of class II molecules from intracellular compartments to the cell surface is dramatically reduced in CatS$^{-/-}$ DC.

Subcellular Distribution of CatS Activity in DC

The wide subcellular distribution of substrates for CatS (p10 in wt DC, p22, p18, and p10 in CatS$^{-/-}$ DC) suggested a corresponding distribution of the active enzyme in mature DC. For direct visualization of CatS activity, we synthesized a derivative of LHVS that carries a phenolic substituent on the vinylsulfone moiety to allow the introduction of ^{125}I (Fig. 9 A). This compound, LHVS-PhOH, was radiolabeled in an Iodogen-catalyzed reaction, and purified by reverse-phase HPLC. The peak fractions of radioactivity were used for labeling experiments. Extracts were prepared from DC obtained either from wt or CatS$^{-/-}$ animals and labeled with ^{125}I–LHVS-PhOH. This comparison immediately revealed the labeled polypeptide of ~28 kD that corresponds to CatS (Fig. 9 B). LHVS-PhOH behaved similarly to LHVS with respect to substrate specificity and affinity, as revealed by competition experiments (data not shown). Using ^{125}I–LHVS-PhOH significant CatS activity was demonstrated in all three subcellular fractions (peaks A, B, and C) of wt DC, while CatS$^{-/-}$ DC showed no detectable signal for active CatS (Fig. 9 C). Therefore, CatS activity is not restricted to late endocytic compartments, but is found along the entire endocytic route in mature DC, in good agreement with the wide pH range of CatS activity in vitro (Chapman et al., 1997). This result is consistent with the presence of substrates of CatS and conversion of αβl into αβm in all endocytic compartments examined (see above).

The additional polypeptides seen in Fig. 9 C most likely represent other cysteine proteases, as the vinyl sulfone functionality of LHVS-PhOH is reactive toward active site cysteines. Furthermore, not only are the mature cathepsins labeled with these probes, but some of their proforms can also be decorated (Bryant R.A.R., and H.L. Ploegh, manuscript in preparation). Some of the higher molecular weight polypeptides are absent in the CatS$^{-/-}$ sample and may indeed correspond to proCatS, which would be in good agreement with a localization in the Golgi–ER compartment represented in peak C.

The pattern of labeling appeared highly pH-dependent, such that at near-neutral pH, excellent selectivity of labeling was obtained. At more acidic pH, a newly labeled species became prominent that we could identify as CatB,

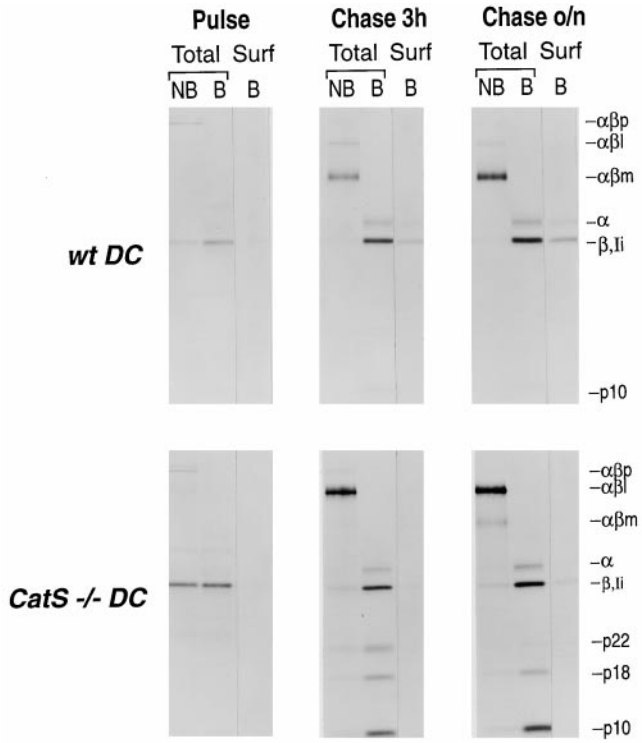

Figure 8. Surface labeling of MHC class II molecules in DC from wt and CatS$^{-/-}$ cells. Flt3-induced DC from wt (upper panels) and CatS$^{-/-}$ (lower panels) mice were pulsed with [^{35}S]cysteine/methionine for 60 min, and chased 3 h and overnight (o/n), respectively. At each chase point the cell surface was biotinylated as described. The samples were immunoprecipitated with N22 to retrieve total cellular MHC class II. 10% of this immunoprecipitate was divided into two and loaded on a SDS-PAGE without or with prior boiling (total, NB, and B). The remaining 90% were reimmunoprecipitated with streptavidin-agarose beads, extensively washed, and analyzed on the same 12.5% SDS-PAGE after boiling (surf, surface; B, boiled).

based on comparison with DC obtained from CatB$^{-/-}$ mice (data not shown). We conclude that LHVS-PhOH is a selective, but by no means uniquely specific probe for CatS, and infer from this result that LHVS can inhibit not only CatS, but also other thiol proteases.

Discussion

The identification of proteases involved in the degradation of Ii in living cells has relied largely on the use of class-specific protease inhibitors, and more recently, on the use of mice genetically deficient in the lysosomal proteases CatD, CatB, CatL, and CatS. Earlier work that implicated CatB and CatD in both Ii degradation and generation of antigenic peptides (van Noort and van der Drift, 1989; Maric et al., 1994; Rodriguez and Diment, 1995) has been superseded by analyses of CatB- and CatD-deficient mice (Deussing et al., 1998). In living cells, neither protease is essential for maturation of class II molecules or antigen presentation. Results obtained with the inhibitor LHVS, rather specific for CatS at low concentrations, implicated CatS in removal of Ii (Riese et al., 1996). In the presence of LHVS, proteolytic processing of Ii is arrested at intermediate stages (Villadangos et al., 1997). As expected, LHVS severely compromises peptide loading, as assessed in pulse–chase experiments. Our data obtained with a radiolabeled version of the LHVS analogue LHVS-PhOH used as an active site–directed probe allowed the identification of enzymatically active CatS, demonstrated its presence throughout the endocytic pathway, and indicated that CatS could act on class II–associated Ii at these different locations. Although LHVS is quite specific for CatS at low concentrations in vitro, higher concentrations of LHVS will readily target other thiol proteases (Bryant, R.A.R., G.-P. Shi, H.A. Chapman, and H.L. Ploegh, unpublished observations), not all of which have been identified to date. CatS$^{-/-}$–deficient mice allow the analysis of the contribution of CatS to maturation and intracellular trafficking of MHC class II independently of the use of pharmacological inhibitors.

Whereas class II maturation has been analyzed biochemically in CatS$^{-/-}$ mice, the contribution of CatS to proper trafficking of class II molecules had not been addressed in this model (Nakagawa et al., 1999; Shi et al., 1999). However, a role for CatS in such control was made plausible in experiments in which the trafficking of class II products was examined in DC in the presence and absence of LHVS (Pierre and Mellman, 1998).

DC are the most potent antigen-presenting cells described to date and represent a rather heterogeneous set of professional APCs that share certain characteristic features (Banchereau and Steinman, 1998). However, bone marrow–derived DC, as generated by incubating bone marrow cells with GM-CSF in vitro, and flt3 ligand–induced splenic DC used in this study, differ in size and relative distribution of marker enzymes. Immature DC, upon encounter with antigen, efficiently internalize and convert the foreign material into class II–peptide complexes. In response to inflammatory stimuli, presumably coincident with acquisition of antigenic material, these DC undergo maturation, in essence externalizing and freezing class II–peptide complexes at the surface for maximal exposure to T cells (Cella et al., 1997). These processes, proposed to be at least in part under the control of CatS, march in lockstep with migration of DC from the periphery to lymph nodes, where contact with T cells occurs. However, the low levels of class II expression on the surface of immature wt DC (Cella et al., 1997), versus the high class II expression on mature DC from CatS$^{-/-}$ mice (Nakagawa et al., 1999; this paper) is a discrepancy that shows differential activity of CatS to be not the only major regulating factor for surface expression of class II during DC maturation.

Application of the inhibitor LHVS to mature DC resulted in an intracellular distribution of class II molecules highly reminiscent of that seen in immature DC. What is the actual route taken by class II molecules in DC and what is the step controlled by the activity of CatS? Class II molecules reach the endocytic compartment either by internalization from the cell surface or by targeting from the TGN, probably to the early endosomal–late endosomal junction. The intracellular localization of CatS activity and the site of conversion of its substrate (αβl into αβm) in DC can provide important information to resolve these ques-

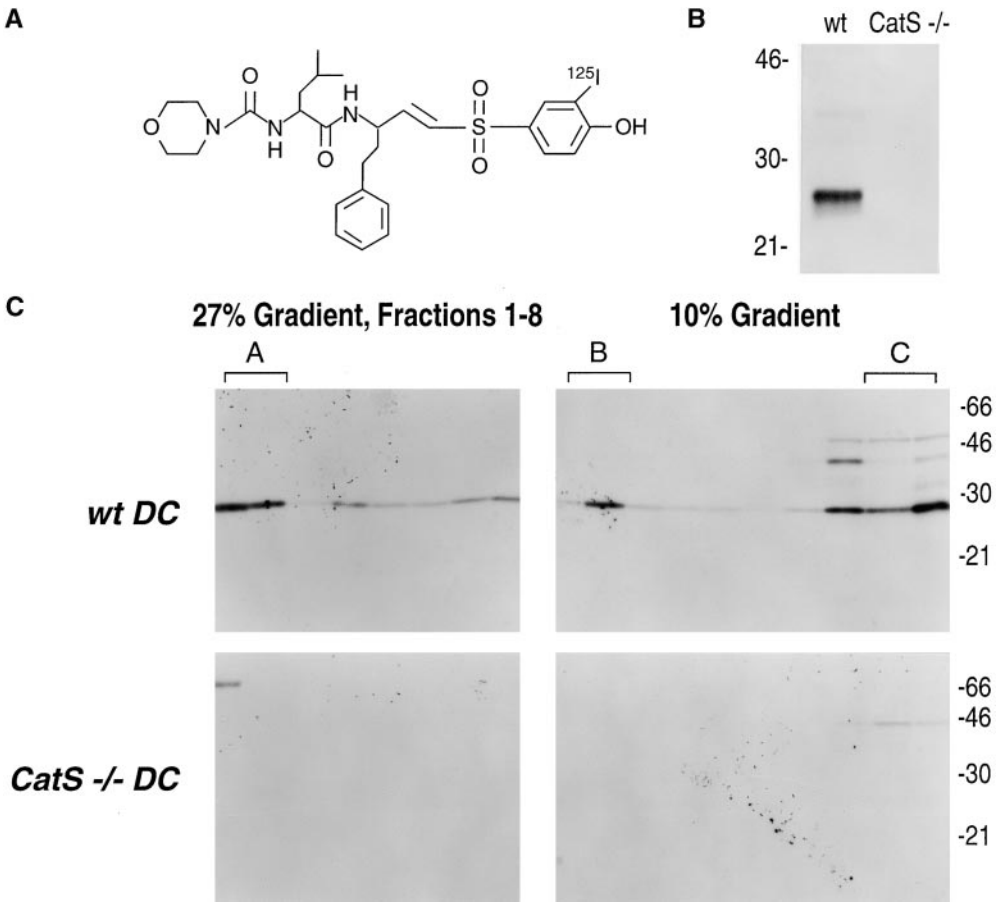

Figure 9. ^{125}I–LHVS-PhOH as a new active site–directed probe to visualize enzymatically active CatS. (A) Structure of ^{125}I–LHVS-PhOH. (B) DC from wt and CatS$^{-/-}$ mice were labeled with ^{125}I–LHVS-PhOH. Active CatS was visualized after separation on SDS-PAGE. (C) Subcellular distribution of active CatS. DC from wt and CatS$^{-/-}$ were subjected to subcellular fractionation as described (see Fig. 3 A). Fractions 1–8 of the 27% Percoll gradient (including the lysosomal peak A) and the entire 10% Percoll gradient (separating late endosomes [peak B] from the remainder [peak C]) were labeled with ^{125}I–LHVS-PhOH, separated by 12.5% SDS-PAGE, and visualized by autoradiography (left panel, high-density fractions 1–8 including peak A; right panel, 10% Percoll gradient of the low density fractions, peak B, and peak C; upper panel, wild-type DC; lower panel, CatS$^{-/-}$ DC).

tions. Using a less direct assay, CatS activity could be demonstrated only in lysosomal compartments of bone marrow–derived DC (Pierre and Mellman, 1998). This contrasts with the broad distribution of CatS activity observed here.

CatS is active throughout the endocytic pathway, as demonstrated both by active site–labeling of CatS and analysis of degradation intermediates of Ii in the presence or absence of CatS. NH_2-terminal processing of Ii by CatS occurred throughout the entire endocytic route in mature DC, whereas COOH-terminal degradation by proteases other than CatS appears to be restricted to nonlysosomal compartments. In the absence of CatS, the NH_2 terminus of Ii retains a sizable fraction of class II molecules in endocytic compartments until it reaches lysosomes. This situation applies to DC as well as splenocytes (Driessen, C., unpublished observations).

The sorting event that directs class II molecules to the cell surface in mature DC was suggested to be localized to an early endocytic compartment, where active CatS would cleave Ii and release the NH_2-terminal sorting signal of Ii from the class II–Ii complexes (Pierre and Mellman, 1998). Class II molecules from that location would reach the cell surface, bypassing later endocytic structures. Alternatively, and at the other end of the spectrum, class II molecules may reach the lysosomal compartment largely independently from the activity of CatS. CatS would then control the egress of class II molecules from lysosomes. We envision that these two extreme possibilities would result in major differences in terms of peptide loading, because of the distinct characteristics of the subcellular compartments encountered by class II molecules before reaching the cell surface in either model. While our data are compatible with either model, they suggest that there are major factors in addition to CatS activity that control the trafficking of class II molecules in DC. After 3 h of chase, we detect a substantial amount of fully mature class II molecules in lysosomal compartments of wt DC, indicating that conversion of Iip 10 into CLIP is probably not the rate-limiting step in directing class II to the PM.

Since αβ–peptide complexes can thus be generated along the entire endocytic route in mature DC, they might leave the endocytic compartment from these many locations independently rather than following a single, shared track. The amount of mature αβ–peptide material retrieved from the cell surface and/or early endosome fraction after 3 h of chase by far exceeds that of any of its precursor forms in a single compartment at a given time. This would support the hypothesis that class II molecules at the surface are recruited from several subcellular compartments. The sizable amount of αβm retrieved from the lysosomal compartment after 3 h of chase contrasts with the smaller amount retrieved under steady-state conditions. We suggest it represents a kinetic intermediate and similarly contributes to the fraction that reaches the surface. Delivery of class II molecules from lysosomes directly to

the cell surface has been suggested (Wubbolts et al., 1996; Thery et al., 1998). The ensuing exchange of CLIP for antigenic peptides necessitates an interaction with H2-DM. Furthermore, peptide cargo directly affects intracellular transport of class II molecules (Bryant et al., 1999). Alternatively, all αβm may traffic to late endocytic or lysosomal compartments before an additional signal is required to release class II to the surface. Again, the impact of interactions with accessory molecules (H2-DM, H2-DO) remains to be assessed.

Breakdown intermediates of Ii are abundant in CatS$^{-/-}$ DC. These intermediates are detected first in early endocytic compartments but are particularly prominent in late endocytic compartments and lysosomes. Based on their molecular mass and the epitopes present, as well as the temporal relationships in the occurrence of these intermediates, a precursor-product relationship was established that could be related to their intracellular location. Iip10, Iip22, and Iip18 accumulate in CatS$^{-/-}$ DC, and therefore are dependent on CatS activity for further processing. They were present in different relative amounts in early and late endocytic compartments. Whereas p22 preferentially was found in early and late endosomes, the p18 form was favored in lysosomal compartments. Therefore, the nature of the CatS substrate(s) changes gradually along the endocytic route. The enzyme(s) involved in conversion of Ii into p22 and p18 have not been identified. In contrast to CatS$^{-/-}$ DC, no accumulation of Iip22 and Iip18 was observed when CatS activity was inhibited by treatment with LHVS in wt DC (making the limitations of the use of this pharmacological inhibitor evident). The incomplete block of CatS activity by LHVS, as demonstrated by this comparison, could be explained by a possible loss of LHVS specificity under the acidic conditions that prevail in late endocytic compartments. Indeed, results obtained with the radiolabeled derivative of LHVS, LHVS-PhOH, showed excellent selectivity of label under neutral conditions rapidly lost at lower pH. The predominant localization of p18 and p22 in late endocytic compartments would be in line with this explanation. Under normal circumstances, the activity of CatS presumably coincides with that of other enzymes that attack Ii, but at present their individual contributions cannot be distinguished.

There is of course a paradox: how can the intracellular retention of MHC class II molecules be reconciled with unaltered levels of surface-expressed class II complexes observed in CatS$^{-/-}$ DC? This puzzle could be resolved if the following conditions apply. First, the half-life of class II at the cell surface must exceed by far the normal rate of surface deposition of class II molecules. There is ample support for this suggestion; peptide-loaded class II complexes are extraordinarily stable (Neefjes and Ploegh, 1992; Cella et al., 1997; Pierre et al., 1997). Second, a homeostatic mechanism that limits the number of class II molecules that can be inserted at the cell surface might be operative. Given sufficient time, even a slow rate of surface deposition, coupled to an upper limit for the number of class II molecules allowed at the cell surface, would result in comparable levels of surface-expressed MHC class II. Relative to their CatS$^{-/-}$ counterparts, in normal DC any surplus of class II molecules might be destroyed, for example in lysosomes, rather than reach the cell surface. This suggestion is consistent with the reproducibly higher recovery of total class II molecules from CatS$^{-/-}$ DC, whereas the recovery of class I molecules is comparable.

Proteolysis of Ii is a compound reaction that controls intracellular transport of MHC class II molecules, and ultimately, their loading with peptide and display at the cell surface. Therefore, class II molecules must function not only at the cell surface, but also in a lysosomal environment. There, the class II–associated Ii chain represents the equivalent of a propiece that keeps MHC class II molecules in an inactive form until Ii is released by proteolysis and its remnants have been cleared from the class II peptide-binding cleft by accessory proteins such as H2-DM. Removal of Ii is a process of interest not only for its immunological consequences but also because proteolytic destruction of Ii is one of the few examples in which proteolysis controls trafficking of a surface glycoprotein. Such controlled proteolysis appears to regulate molecular trafficking and maturation of at least three other transmembrane proteins, the Notch receptor (Logeat et al., 1998; De Strooper et al., 1999), the sterol regulatory element binding protein SREBP (Brown and Goldstein, 1997), and β-amyloid precursor protein APP (De Strooper et al., 1999; Wolfe et al., 1999). For all three of these proteins, two or three consecutive proteolytical steps are suggested to occur in a sequential fashion, culminating in the release of an effector molecule (in these cases a protein fragment) that traffics from the PM to either the nucleus (Notch, SREBP) or the extracellular environment (APP) (Chan and Jan, 1998). The proteases that perform this final cleavage and therefore largely control the biological activity of the cleaved substrates have not been identified. The regulation of MHC class II trafficking by sequential degradation of Ii, as unraveled using DC from CatS$^{-/-}$ mice in this study, is not unlike these models: at least two proteolytic steps, one of which is performed by CatS, occur in a sequential fashion in the course of Ii degradation along the endocytic route. This late step releases the αβ–CLIP complex and initiates loading with antigenic peptide to generate the biologically active entity. Unlike the known examples for the control of trafficking and maturation of transmembrane proteins by sequential proteolysis, degradation of Ii does not occur in the cytosol but in late endocytic compartments where multiple proteolytic enzymes with partly overlapping functions and specificities are concentrated. Even in the lysosomal environment, rich in a large selection of proteases, proteolytic enzymes afford sufficient specificity to tightly regulate essential cellular properties.

The authors thank N. Mach and G. Dranoff for generously providing the flt3 ligand–transfected melanoma cells and K.V. Figura and P. Pierre for their gifts of antisera.

This work was supported by Deutsche Forschungsgemeinschaft (DR 378/1-1 to C. Driessen), the Cancer Research Institute (R.A.R. Bryant), l'Association Française pour la Recherche Thérapeutique (A.-M. Lennon-Duménil), the Lady Tata Foundation (J.A. Villadangos), Boehringer-Ingelheim Pharmaceuticals, Inc. (H.L. Ploegh), and the National Institutes of Health (AI34893 and CA14051 to H.L. Ploegh; HL48261 to H.A. Chapman; and HL60942 to G.-P. Shi).

Submitted: 6 July 1999
Revised: 22 September 1999
Accepted: 1 October 1999

References

Amigorena, S., P. Webster, J. Drake, J. Newcomb, P. Cresswell, and I. Mellman. 1995. Invariant chain cleavage and peptide loading in major histocompatibility complex class II vesicles. *J. Exp. Med.* 181:1729–1741.

Bakke, O., and B. Dobberstein. 1990. MHC class II-associated invariant chain contains a sorting signal for endosomal compartments. *Cell.* 63:707–716.

Banchereau, J., and R.M. Steinman. 1998. Dendritic cells and the control of immunity. *Nature.* 392:245–252.

Bijlmakers, M.J., P. Benaroch, and H.L. Ploegh. 1994. Mapping functional regions in the lumenal domain of the class II-associated invariant chain. *J. Exp. Med.* 180:623–629.

Brown, M.S., and J.L. Goldstein. 1997. The SREBP pathway: regulation of cholesterol metabolism by proteolysis of a membrane-bound transcription factor. *Cell.* 89:331–340.

Bryant, P.W., P. Roos, H.L. Ploegh, and A.J. Sant. 1999. Deviant trafficking of I-Ad mutant molecules is reflected in their peptide binding properties. *Eur. J. Immunol.* 29:2729–2739.

Castellino, F., and R.N. Germain. 1995. Extensive trafficking of MHC class II-invariant chain complexes in the endocytic pathway and appearance of peptide-loaded class II in multiple compartments. *Immunity.* 2:73–88.

Cella, M., A. Engering, V. Pinet, J. Pieters, and A. Lanzavecchia. 1997. Inflammatory stimuli induce accumulation of MHC class II complexes on dendritic cells. *Nature.* 388:782–787.

Chan, Y.M., and Y.N. Jan. 1998. Roles for proteolysis and trafficking in notch maturation and signal transduction. *Cell.* 94:423–426.

Chapman, H.A. 1998. Endosomal proteolysis and MHC class II function. *Curr. Opin. Immunol.* 10:93–102.

Chapman, H.A., R.J. Riese, and G.-P. Shi. 1997. Emerging roles for cysteine proteases in human biology. *Annu. Rev. Physiol.* 59:63–88.

De Strooper, B., W. Annaert, P. Cupers, P. Saftig, K. Craessaerts, J.S. Mumm, E.H. Schroeter, V. Schrijvers, M.S. Wolfe, W.J. Ray, A. Goate, and R. Kopan. 1999. A presenilin-1-dependent gamma-secretase-like protease mediates release of Notch intracellular domain. *Nature.* 398:518–522.

Demotz, S., H.M. Grey, E. Appella, and A. Sette. 1989a. Characterization of a naturally processed MHC class II-restricted T-cell determinant of hen egg lysozyme. *Nature.* 342:682–684.

Demotz, S., P.M. Matricardi, C. Irle, P. Panina, A. Lanzavecchia, and G. Corradin. 1989b. Processing of tetanus toxin by human antigen-presenting cells. Evidence for donor and epitope-specific processing pathways. *J. Immunol.* 143:3881–3886.

Denzin, L.K., and P. Cresswell. 1995. HLA-DM induces CLIP dissociation from MHC class II alpha beta dimers and facilitates peptide loading. *Cell.* 82:155–165.

Deussing, J., W. Roth, P. Saftig, C. Peters, H.L. Ploegh, and J.A. Villadangos. 1998. Cathepsins B and D are dispensable for major histocompatibility complex class II-mediated antigen presentation. *Proc. Natl. Acad. Sci. USA.* 95: 4516–4521.

Germain, R.N. 1994. MHC-dependent antigen processing and peptide presentation: providing ligands for T lymphocyte activation. *Cell.* 76:287–299.

Ghosh, P., M. Amaya, E. Mellins, and D.C. Wiley. 1995. The structure of an intermediate in class II MHC maturation: CLIP bound to HLA-DR3. *Nature.* 378:457–462.

Green, S.A., K.P. Zimmer, G. Griffiths, and I. Mellman. 1987. Kinetics of intracellular transport and sorting of lysosomal membrane and plasma membrane proteins. *J. Cell Biol.* 105:1227–1240.

Heemels, M.T., and H. Ploegh. 1995. Generation, translocation, and presentation of MHC class I-restricted peptides. *Annu. Rev. Biochem.* 64:463–491.

Inaba, K., M. Inaba, N. Romani, H. Aya, M. Deguchi, S. Ikehara, S. Muramatsu, and R.M. Steinman. 1992. Generation of large numbers of dendritic cells from mouse bone marrow cultures supplemented with granulocyte/macrophage colony-stimulating factor. *J. Exp. Med.* 176:1693–1702.

Kleijmeer, M.J., S. Morkowski, J.M. Griffith, A.Y. Rudensky, and H.J. Geuze. 1997. Major histocompatibility complex class II compartments in human and mouse B lymphoblasts represent conventional endocytic compartments. *J. Cell Biol.* 139:639–649.

Logeat, F., C. Bessia, C. Brou, O. LeBail, S. Jarriault, N.G. Seidah, and A. Israel. 1998. The Notch1 receptor is cleaved constitutively by a furin-like convertase. *Proc. Natl. Acad. Sci. USA.* 95:8108–8112.

Lotteau, V., L. Teyton, A. Peleraux, T. Nilsson, L. Karlsson, S.L. Schmid, V. Quaranta, and P.A. Peterson. 1990. Intracellular transport of class II MHC molecules directed by invariant chain. *Nature.* 348:600–605.

Lotze, M.T., and A. Thompson. 1999. Dendritic Cells: Biology and Clinical Applications. Academic Press, San Diego, CA. 733 pp.

Mane, S.M., L. Marzella, D.F. Bainton, V.K. Holt, Y. Cha, J.E. Hildreth, and J.T. August. 1989. Purification and characterization of human lysosomal membrane glycoproteins. *Arch. Biochem. Biophys.* 268:360–378.

Maraskovsky, E., K. Brasel, M. Teepe, E.R. Roux, S.D. Lyman, K. Shortman, and H.J. McKenna. 1996. Dramatic increase in the numbers of functionally mature dendritic cells in Flt3 ligand-treated mice: multiple dendritic cell subpopulations identified. *J. Exp. Med.* 184:1953–1962.

Maraskovsky, E., B. Pulendran, K. Brasel, M. Teepe, E.R. Roux, K. Shortman, S.D. Lyman, and H.J. McKenna. 1997. Dramatic numerical increase of functionally mature dendritic cells in FLT3 ligand-treated mice. *Adv. Exp. Med. Biol.* 417:33–40.

Maric, M.A., M.D. Taylor, and J.S. Blum. 1994. Endosomal aspartic proteinases are required for invariant-chain processing. *Proc. Natl. Acad. Sci. USA.* 91: 2171–2175.

Martin, W.D., G.G. Hicks, S.K. Mendiratta, H.I. Leva, H.E. Ruley, and L. Van Kaer. 1996. H2-M mutant mice are defective in the peptide loading of class II molecules, antigen presentation, and T cell repertoire selection. *Cell.* 84: 543–550.

Metlay, J.P., M.D. Witmer-Pack, R. Agger, M.T. Crowley, D. Lawless, and R.M. Steinman. 1990. The distinct leukocyte integrins of mouse spleen dendritic cells as identified with new hamster monoclonal antibodies. *J. Exp. Med.* 171:1753–1771.

Miyazaki, T., P. Wolf, S. Tourne, C. Waltzinger, A. Dierich, N. Barois, H. Ploegh, C. Benoist, and D. Mathis. 1996. Mice lacking H2-M complexes, enigmatic elements of the MHC class II peptide-loading pathway. *Cell.* 84: 531–541.

Nakagawa, T.Y., W.H. Brissette, P.D. Lira, R.J. Griffiths, N. Petrushova, J. Stock, J.D. McNeish, S.E. Eastman, E.D. Howard, S.R. Clarke, et al. 1999. Impaired invariant chain degradation and antigen presentation and diminished collagen-induced arthritis in cathepsin S null mice. *Immunity.* 10:207–217.

Neefjes, J.J., and H.L. Ploegh. 1992. Inhibition of endosomal proteolytic activity by leupeptin blocks surface expression of MHC class II molecules and their conversion to SDS resistance alpha beta heterodimers in endosomes. *EMBO (Eur. Mol. Biol. Organ.) J.* 11:411–416.

Newcomb, J.R., and P. Cresswell. 1993. Structural analysis of proteolytic products of MHC class II-invariant chain complexes generated in vivo. *J. Immunol.* 151:4153–4163.

Palmer, J.T., D. Rasnick, J.L. Klaus, and D. Bromme. 1995. Vinyl sulfones as mechanism-based cysteine protease inhibitors. *J. Med. Chem.* 38:3193–3196.

Pierre, P., and I. Mellman. 1998. Developmental regulation of invariant chain proteolysis controls MHC class II trafficking in mouse dendritic cells. *Cell.* 93:1135–1145.

Pierre, P., S.J. Turley, E. Gatti, M. Hull, J. Meltzer, A. Mirza, K. Inaba, R.M. Steinman, and I. Mellman. 1997. Developmental regulation of MHC class II transport in mouse dendritic cells. *Nature.* 388:787–792.

Pieters, J. 1997. MHC class II restricted antigen presentation. *Curr. Opin. Immunol.* 9:89–96.

Ploegh, H.L. 1995. Trafficking and assembly of MHC molecules: how viruses elude the immune system. *Cold Spring Harbor Symp. Quant. Biol.* 60:263–266.

Riese, R.J., P.R. Wolf, D. Bromme, L.R. Natkin, J.A. Villadangos, H.L. Ploegh, and H.A. Chapman. 1996. Essential role for cathepsin S in MHC class II-associated invariant chain processing and peptide loading. *Immunity.* 4:357–366.

Riese, R.J., R.N. Mitchell, J.A. Villadangos, G.-P. Shi, J.T. Palmer, E.R. Karp, G.T. De Sanctis, H.L. Ploegh, and H.A. Chapman. 1998. Cathepsin S activity regulates antigen presentation and immunity. *J. Clin. Invest.* 101:2351–2363.

Roche, P.A. 1995. HLA-DM: an in vivo facilitator of MHC class II peptide loading. *Immunity.* 3:259–262.

Roche, P.A., and P. Cresswell. 1991. Proteolysis of the class II-associated invariant chain generates a peptide binding site in intracellular HLA-DR molecules. *Proc. Natl. Acad. Sci. USA.* 88:3150–3154.

Rodriguez, G.M., and S. Diment. 1995. Destructive proteolysis by cysteine proteases in antigen presentation of ovalbumin. *Eur. J. Immunol.* 25:1823–1827.

Romagnoli, P., and R.N. Germain. 1994. The CLIP region of invariant chain plays a critical role in regulating major histocompatibility complex class II folding, transport, and peptide occupancy. *J. Exp. Med.* 180:1107–1113.

Rome, L.H., A.J. Garvin, M.M. Allietta, and E.F. Neufeld. 1979. Two species of lysosomal organelles in cultured human fibroblasts. *Cell.* 17:143–153.

Roth, J., and E.G. Berger. 1982. Immunocytochemical localization of galactosyltransferase in HeLa cells: codistribution with thiamine pyrophosphatase in trans-Golgi cisternae. *J. Cell Biol.* 93:223–229.

Shi, G.-P., J.A. Villadangos, G. Dranoff, C. Small, L. Gu, K.J. Haley, R. Riese, H.L. Ploegh, and H.A. Chapman. 1999. Cathepsin S required for normal MHC class II peptide loading and germinal center development. *Immunity.* 10:197–206.

Shurin, M.R., P.P. Pandharipande, T.D. Zorina, C. Haluszczak, V.M. Subbotin, O. Hunter, A. Brumfield, W.J. Storkus, E. Maraskovsky, and M.T. Lotze. 1997. FLT3 ligand induces the generation of functionally active dendritic cells in mice. *Cell. Immunol.* 179:174–184.

Sloan, V.S., P. Cameron, G. Porter, M. Gammon, M. Amaya, E. Mellins, and D.M. Zaller. 1995. Mediation by HLA-DM of dissociation of peptides from HLA-DR. *Nature.* 375:802–806.

Thery, C., V. Brachet, A. Regnault, M. Rescigno, P. Ricciardi-Castagnoli, C. Bonnerot, and S. Amigorena. 1998. MHC class II transport from lysosomal compartments to the cell surface is determined by stable peptide binding, but not by the cytosolic domains of the alpha- and beta-chains. *J. Immunol.* 161:2106–2113.

van Noort, J.M., and A.C. van der Drift. 1989. The selectivity of cathepsin D suggests an involvement of the enzyme in the generation of T-cell epitopes. *J. Biol. Chem.* 264:14159–14164.

Villadangos, J.A., R.J. Riese, C. Peters, H.A. Chapman, and H.L. Ploegh. 1997. Degradation of mouse invariant chain: roles of cathepsins S and D and the influence of major histocompatibility complex polymorphism (published erratum appears in *J. Exp. Med.* 186:5945). *J. Exp. Med.* 186:549–560.

Viville, S., J. Neefjes, V. Lotteau, A. Dierich, M. Lemeur, H. Ploegh, C. Benoist, and D. Mathis. 1993. Mice lacking the MHC class II-associated in-

variant chain. *Cell.* 72:635–648.
Wolf, P.R., and H.L. Ploegh. 1995. How MHC class II molecules acquire peptide cargo: biosynthesis and trafficking through the endocytic pathway. *Annu. Rev. Cell Dev. Biol.* 11:267–306.
Wolfe, M.S., W. Xia, B.L. Ostaszewski, T.S. Diehl, W.T. Kimberly, and D.J. Selkoe. 1999. Two transmembrane aspartates in presenilin-1 required for presenilin endoproteolysis and gamma-secretase activity. *Nature.* 398:513–517.
Wubbolts, R., M. Fernandez-Borja, L. Oomen, D. Verwoerd, H. Janssen, J. Calafat, A. Tulp, S. Dusseljee, and J. Neefjes. 1996. Direct vesicular transport of MHC class II molecules from lysosomal structures to the cell surface. *J. Cell Biol.* 135:611–622.